

RESTRICTED

Copy No.

6

RM No. A8H12

CLASSIFICATION CHANGED UNCLASSIFIED

~~RESTRICTED~~

6 OCT 1948

~~115.5~~

~~NAC-1~~

~~1012-64~~

~~pt. 1~~

~~ca~~

naca Release form
authority of H.L. Dryden
by HQR, 7-10-51
June 27, 1951

NACA

NACA RM No. A8H12

RESEARCH MEMORANDUM

HIGH-SPEED AERODYNAMIC CHARACTERISTICS OF A

LATERAL-CONTROL MODEL. I - NACA 0012-64

SECTION WITH 20-PERCENT-CHORD PLAIN

AILERON AND 0° AND 45° SWEEPBACK

By Joseph L. Anderson and Walter J. Krumm

Ames Aeronautical Laboratory,
Moffett Field, Calif.

CLASSIFICATION CANCELLED

Authority J. W. Crowley Date 12-14-58
VEO 10501

By JH-1-11-54 See naca
RF 1942

This document contains classified information affecting the National Defense of the United States within the meaning of the Espionage Act, USC 5034 and 35. Its transmission or the revelation of its contents in any manner to an unauthorized person is prohibited by law. Information so classified may be imparted only to persons in the military and naval services of the United States, appropriate civilian officers and employees of the Federal Government who have a legitimate interest therein, and to United States citizens of known loyalty and discretion who of necessity must be informed thereof.

NATIONAL ADVISORY COMMITTEE FOR AERONAUTICS

WASHINGTON
September 27, 1948

NACA LIBRARY

LANGLEY MEMORIAL AERONAUTICAL
LABORATORY
Langley Field, Va.

~~RESTRICTED~~

UNCLASSIFIED



UNCLASSIFIED

NATIONAL ADVISORY COMMITTEE FOR AERONAUTICS

RESEARCH MEMORANDUM

HIGH-SPEED AERODYNAMIC CHARACTERISTICS OF A LATERAL-CONTROL

MODEL. I - NACA 0012-64 SECTION WITH 20-PERCENT-CHORD

PLAIN AILERON AND 0° AND 45° SWEEPBACK

By Joseph L. Anderson and Walter J. Krumm

SUMMARY

Wind-tunnel tests were made to determine the aerodynamic characteristics of a 20-percent-chord plain aileron on a semispan wing having the NACA 0012-64 section. This report includes the results of tests of the wing unswept and swept back 45° and with the aileron deflected from 0° to 10° . Data were obtained for a Mach number range from 0.40 to 0.85.

The results with the wing unswept indicated an aileron overbalance and reversal of effectiveness at high speeds. With the wing swept back 45° the aileron exhibited only an overbalance and no reversal of effectiveness.

INTRODUCTION

Work has been done concerning adequate longitudinal control of airplanes at high speeds, but development of adequate lateral control has not kept pace. In order to investigate the problems of lateral control and span loading and to develop ailerons which are effective at high speeds, a semispan wing model was built and tests of the model were made in the Ames 16-foot high-speed wind tunnel.

The model was fitted with a leading-edge aileron and a trailing-edge aileron. This report includes the results of tests of the wing unswept and swept back 45° with a trailing-edge aileron.

UNCLASSIFIED

SYMBOLS

The coefficients and symbols used in this report are defined as follows:

- A aspect ratio $\left(\frac{2b^2}{S}\right)$
 C_D drag coefficient $\left(\frac{D}{qS}\right)$
 C_L lift coefficient $\left(\frac{L}{qS}\right)$
 C_h aileron hinge-moment coefficient $\left(\frac{H}{qc_a^2 b_a}\right)$
 C_l rolling-moment coefficient $\left(\frac{L^r}{4qSb}\right)$
 C_m pitching-moment coefficient $\left(\frac{M^r}{qSc}\right)$
 C_n section normal-force coefficient $\left(\frac{n}{qc}\right)$
M Mach number $\left(\frac{V}{a}\right)$
R Reynolds number $\left(\frac{\rho V c}{\mu}\right)$

where

- D drag of semispan model, pounds
H aileron hinge moment, foot-pounds
L lift of semispan model, pounds
 L^r rolling moment about longitudinal axis parallel to the air stream in plane of symmetry, foot-pounds
 M^r pitching moment about the 0.25 \bar{c} of semispan model, foot-pounds
S area of semispan model, square feet
V velocity of the free air stream, feet per second
a speed of sound in the free air stream, feet per second
b semispan of model, feet

- b_a aileron span parallel to the hinge line, feet
- c chord of wing perpendicular to 0.25 chord line, feet
- \bar{c} mean aerodynamic chord $\left(\frac{\int \text{chord}^2 dy}{\int \text{chord} dy} \right)$, feet
- \bar{c}_a root-mean-square chord of aileron perpendicular to the hinge line, feet
- n section normal force, pounds per foot
- q dynamic pressure $\left(\frac{1}{2} \rho V^2 \right)$, pounds per square foot
- α angle of attack of model, degrees
- δ_a trailing-edge aileron deflection relative to airfoil, positive when the trailing edge is deflected downward, degrees

DESCRIPTION OF MODEL AND APPARATUS

The model (fig. 1) used for these tests was a semispan tapered wing with the NACA 0012-64 section (table I). For the wing unswept the 0.25 wing-chord line was perpendicular to the air stream. For the wing swept back, the wing was rotated about the 0.50 root-chord point so that the 0.25 wing-chord line was 45° to the air stream. The model dimensions for the wing unswept and swept back 45° are given in table II. The wing was fitted with a 15-percent chord, leading-edge, unsealed aileron which was not deflected for this investigation, and a 20-percent-chord, trailing-edge aileron. The trailing-edge aileron extended in span from 0.561 of the semispan of the unswept wing to the tip and had an unsealed radius nose. This aileron was deflected from 0° to 10° for this investigation. The aileron hinge moments were measured with resistance-type electrical strain gages.

The model was mounted in the tunnel with the wing spar extending through the tunnel wall and fastened to the balance frame. A baffle was installed on the model near the tunnel wall to direct the leakage flow through the tunnel wall away from the surface of the model. (See fig. 2.)

Chordwise rows of pressure orifices were located perpendicular to the 0.25 wing-chord line at six spanwise stations: 0.179, 0.417, 0.581, 0.724, 0.867, and 0.935 of the semispan of the unswept wing; so that chordwise and spanwise pressure distributions could be measured.

CORRECTIONS TO DATA

The data were corrected for the blockage of the tunnel air stream by the model. The angle of attack and the drag and rolling-moment coefficients were corrected for the effect of the tunnel walls by the method of reference 1. As a basis for these corrections, the span loading on the wing at 0.80 Mach number was used. The corrections were applied to the data as follows:

$$\alpha = \alpha_u + \Delta\alpha$$

$$C_D = C_{D_u} + \Delta C_D$$

$$C_l = K C_{l_u}$$

where the corrections are given in the following table:

Corrections	Wing unswept	Wing swept back
$\Delta\alpha$, degrees	0.41 C_L	0.51 C_L
ΔC_D	.0064 C_L^2	.0076 C_L^2
K	.902	.910

The subscript u denotes the uncorrected data. No corrections were made for the effect of the tunnel-wall boundary layer passing over the model.

RESULTS AND DISCUSSION

The test Reynolds numbers for the wing unswept and swept back 45° are shown in figure 3. For the wing unswept and swept back, and with the aileron undeflected, the variation of lift coefficient with angle of attack, the variation of drag coefficient with Mach number, and the variation of pitching-moment coefficient with lift coefficient are presented in figures 4, 5, and 6. The Mach number of lift and drag divergence for the wing unswept is about 0.80.

The increment of rolling-moment coefficient produced by deflection of the trailing-edge aileron for the wing unswept and swept back 45° is presented in figure 7. For the wing unswept,

at most angles of attack there is a decrease in aileron effectiveness as the Mach number is increased from 0.60 to 0.85, and at 0.85 Mach number for -4° and -2° angle of attack a positive deflection of the aileron produces negative increments of rolling-moment coefficient. (See fig. 7(a).) The effectiveness is, in general, reduced for the swept wing.

Figure 8 shows the variation of trailing-edge aileron hinge-moment coefficient with aileron deflection for the wing unswept and swept back 45° . At 0.70 Mach number for the wing unswept, the aileron becomes overbalanced at negative angles of attack and the aileron is overbalanced over a greater angle-of-attack range as the Mach number is increased. The aileron, for the wing swept back, is overbalanced at high Mach numbers but not to as great an extent as for the wing unswept. Reference 2 indicates that a trailing-edge angle greater than approximately 14° causes a control surface to overbalance and reverse its effectiveness at high subsonic Mach numbers. The trailing-edge angle parallel to the air stream of the wing unswept is 20.63° , and this large angle might be the cause of the aileron overbalance and effectiveness reversal. Sweeping the wing back reduced the effect of the large trailing-edge angle.

The spanwise variation of section normal-force coefficient for the wing unswept and swept back is presented in figures 9 and 10, respectively. These data were obtained from integration of the chordwise pressure distribution (normal to the 0.25-wing chord) at each of six spanwise stations. For the wing unswept, the loss of lift on the wing at about 55 percent of the wing semispan is probably the result of leakage around the inboard ends of the ailerons. For the wing swept back, there is no indication of this loss of lift.

Ames Aeronautical Laboratory,
National Advisory Committee for Aeronautics,
Moffett Field, Calif.

REFERENCES

1. Sivells, James C., and Deters, Owen J.: Jet-Boundary and Plan-Form Corrections for Partial-Span Models with Reflection Plane, End Plate, or No End Plate in a Closed Circular Wind Tunnel. NACA TN No. 1077, 1946.

2. Axelson, John A.: A Summary and Analysis of Wind-Tunnel Data on the Lift and Hinge-Moment Characteristics of Control Surfaces up to a Mach Number of 0.90. NACA RM No. A7L02, 1947.

TABLE I. -- COORDINATES IN PERCENT CHORD
FOR NACA 0012-64 SECTION

Station	Ordinate
0.00	0.00
1.25	1.81
2.50	2.45
5.00	3.27
7.50	3.81
10.00	4.24
15.00	4.87
20.00	5.29
30.00	5.83
40.00	6.00
50.00	5.83
60.00	5.32
70.00	4.48
80.00	3.32
90.00	1.87
95.00	1.03
100.00	0.12

L.E. radius: 1.58
T.E. angle: 20.63°



TABLE II. - MODEL DIMENSIONS

Dimension	Unswapt wing	Swept-back wing
Semispan area, square feet	12.25	12.35
Semispan, feet	7.00	5.327
Aspect ratio (based on full span)	8.00	4.59
Taper ratio	0.50	0.484
Sweepback of leading edge, degrees	2.415	47.415
Sweepback of 0.25 chord line, degrees	0	45
Sweepback of trailing edge, degrees	-7.206	37.794
Mean aerodynamic chord, feet	1.841	2.513
Root chord, feet	2.360	3.224
Projected tip chord, feet	1.180	1.559
Leading-edge aileron:		
Ratio of aileron chord to wing chord (perpendicular to quarter-chord line)	0.15	0.15
Span along hinge-line, feet	2.445	2.445
Root-mean-square chord of aileron, feet	0.224	0.224
Trailing-edge aileron:		
Ratio of aileron chord to wing chord (perpendicular to quarter-chord line)	0.20	0.20
Span along hinge line, feet	2.998	2.998
Root-mean-square chord of aileron, feet	0.312	0.312

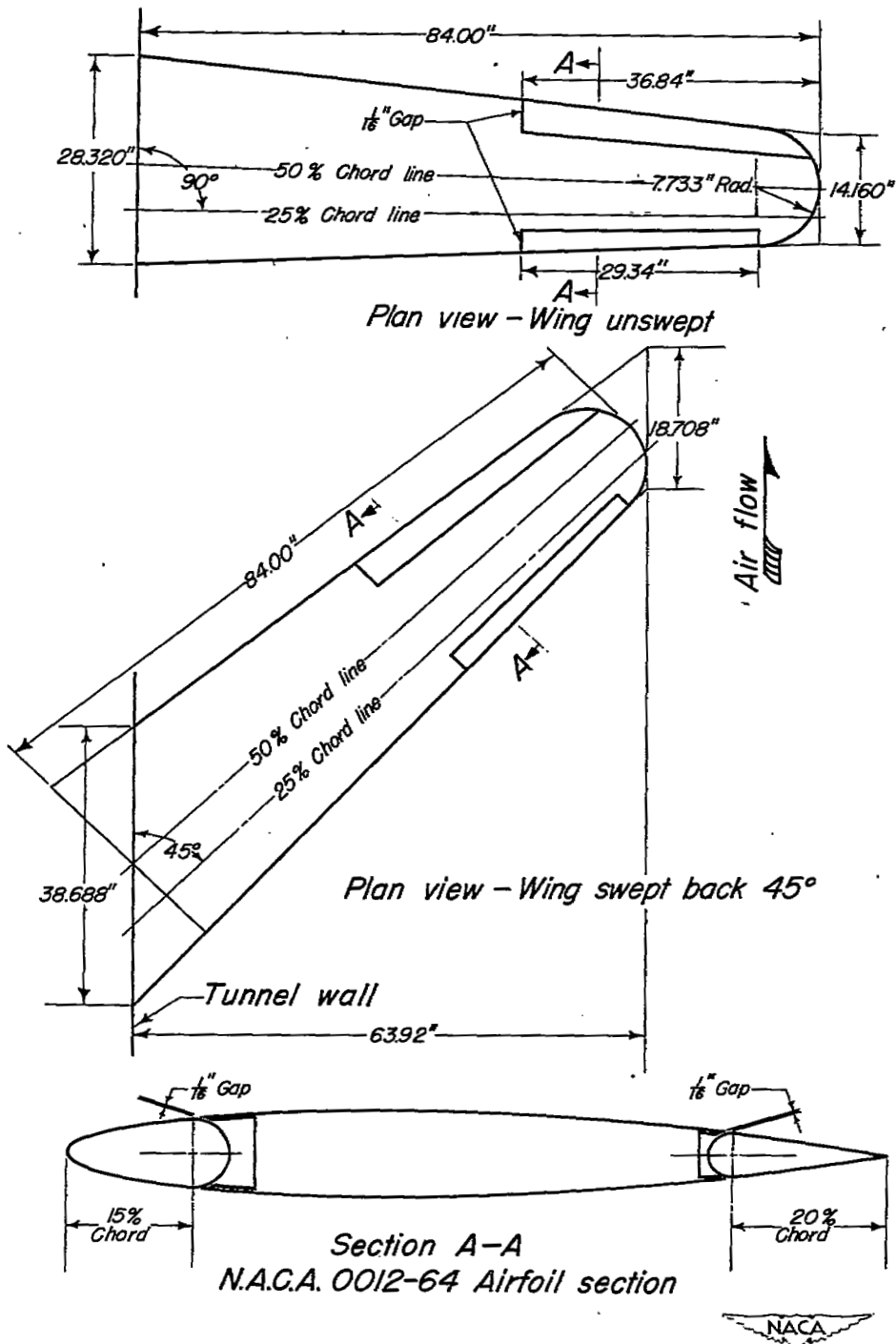
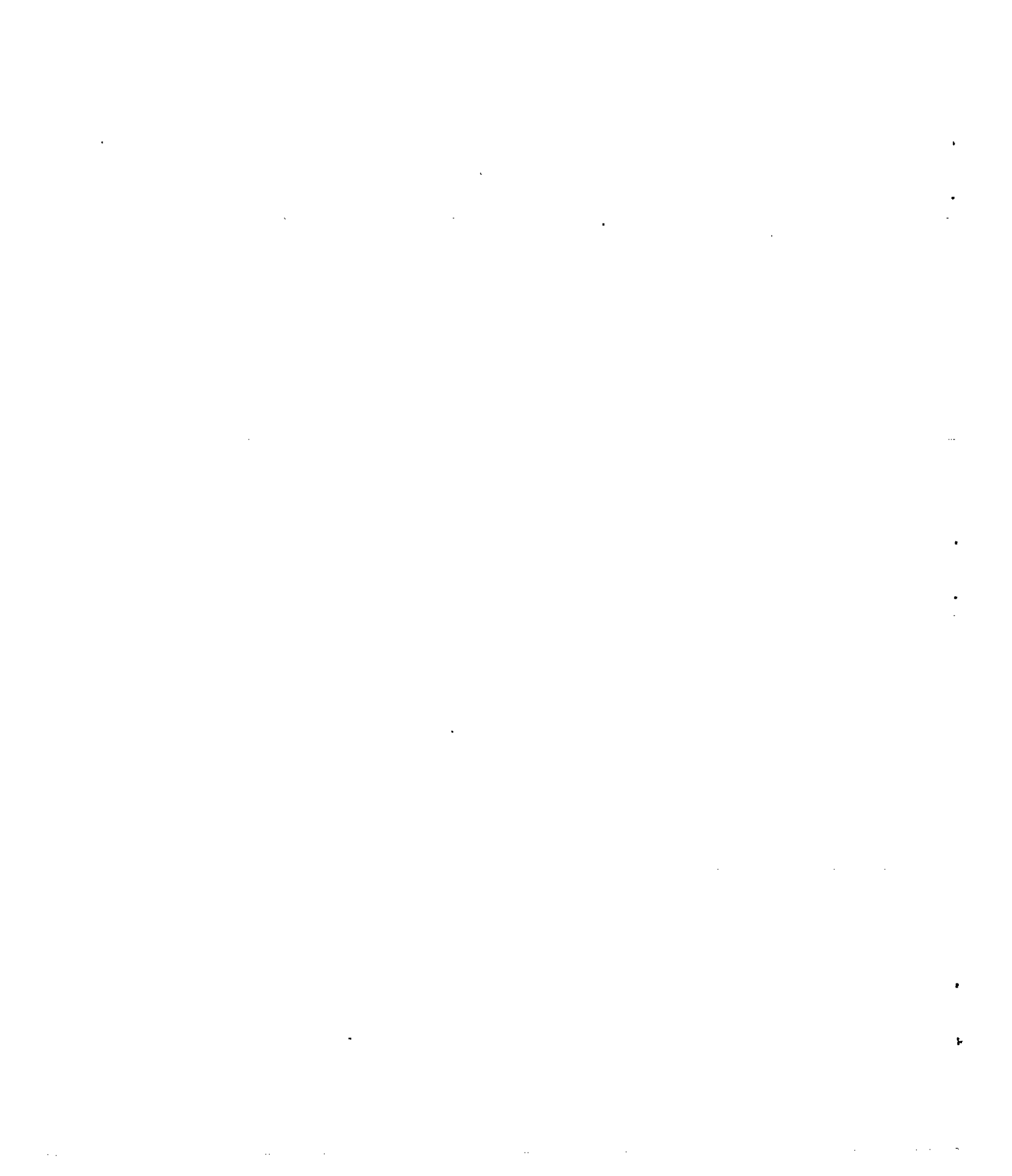


Figure 1.-Lateral control development model.



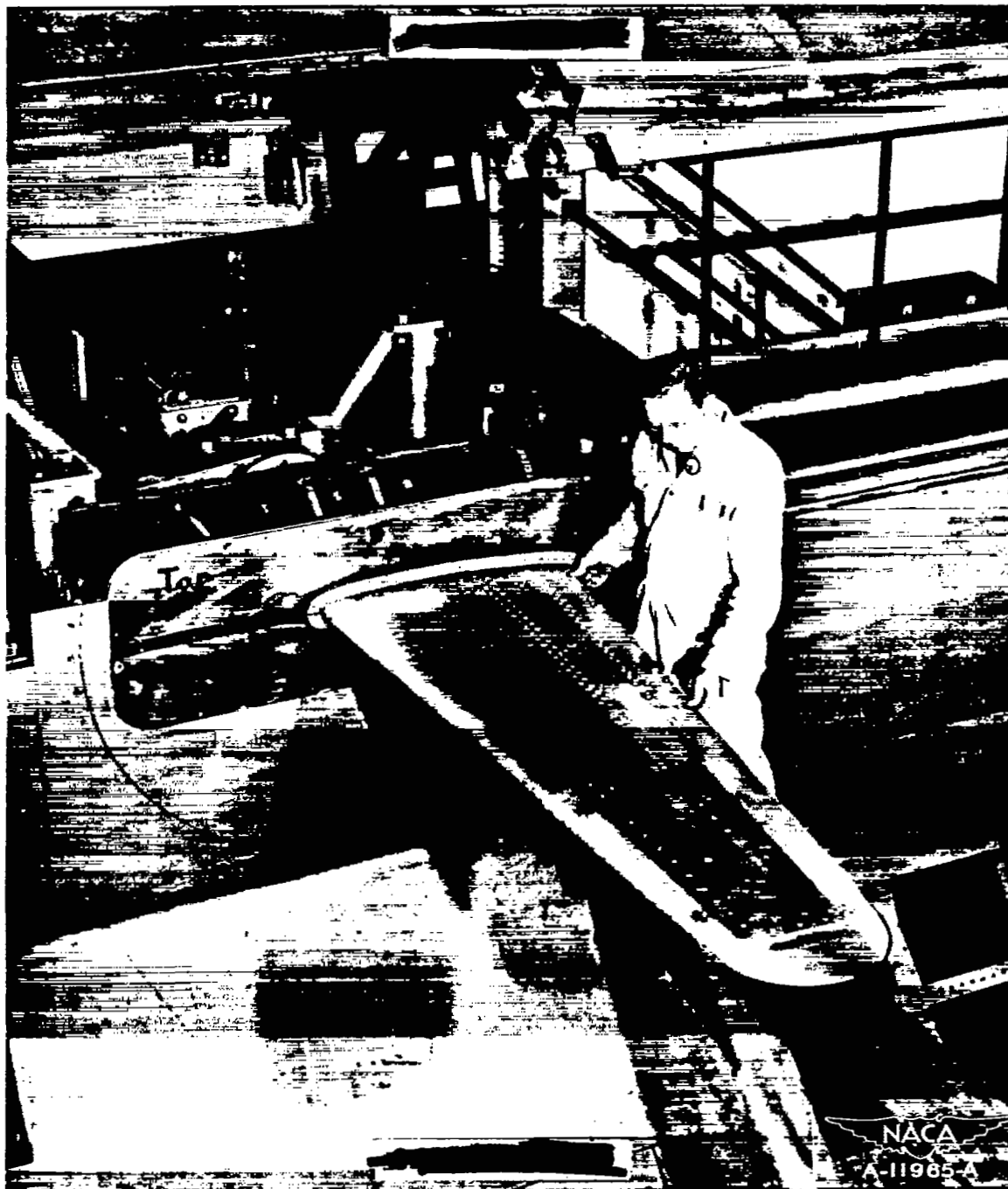


Figure 2. - Unswept wing mounted in the Ames 16-foot high-speed wind tunnel.



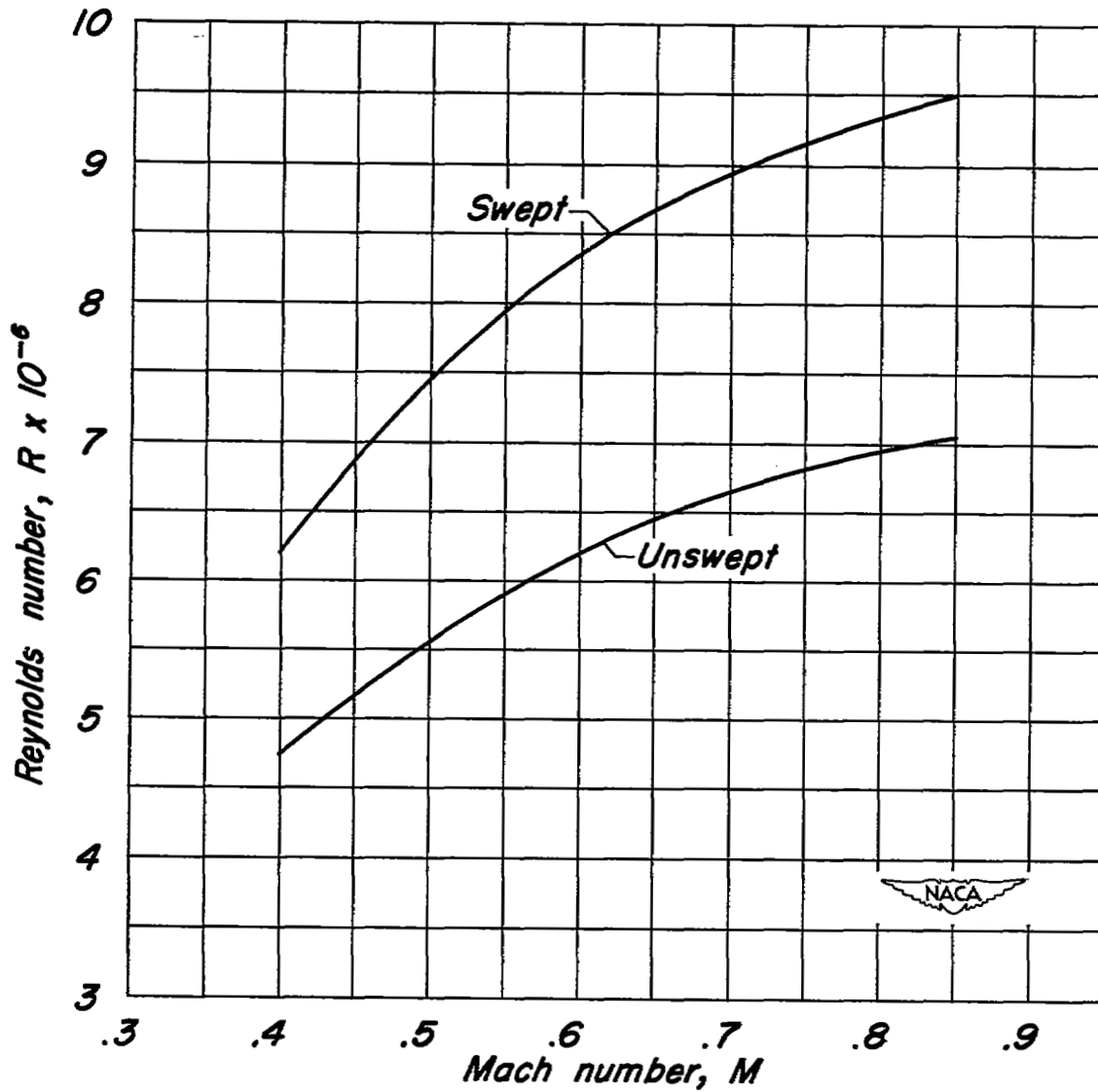
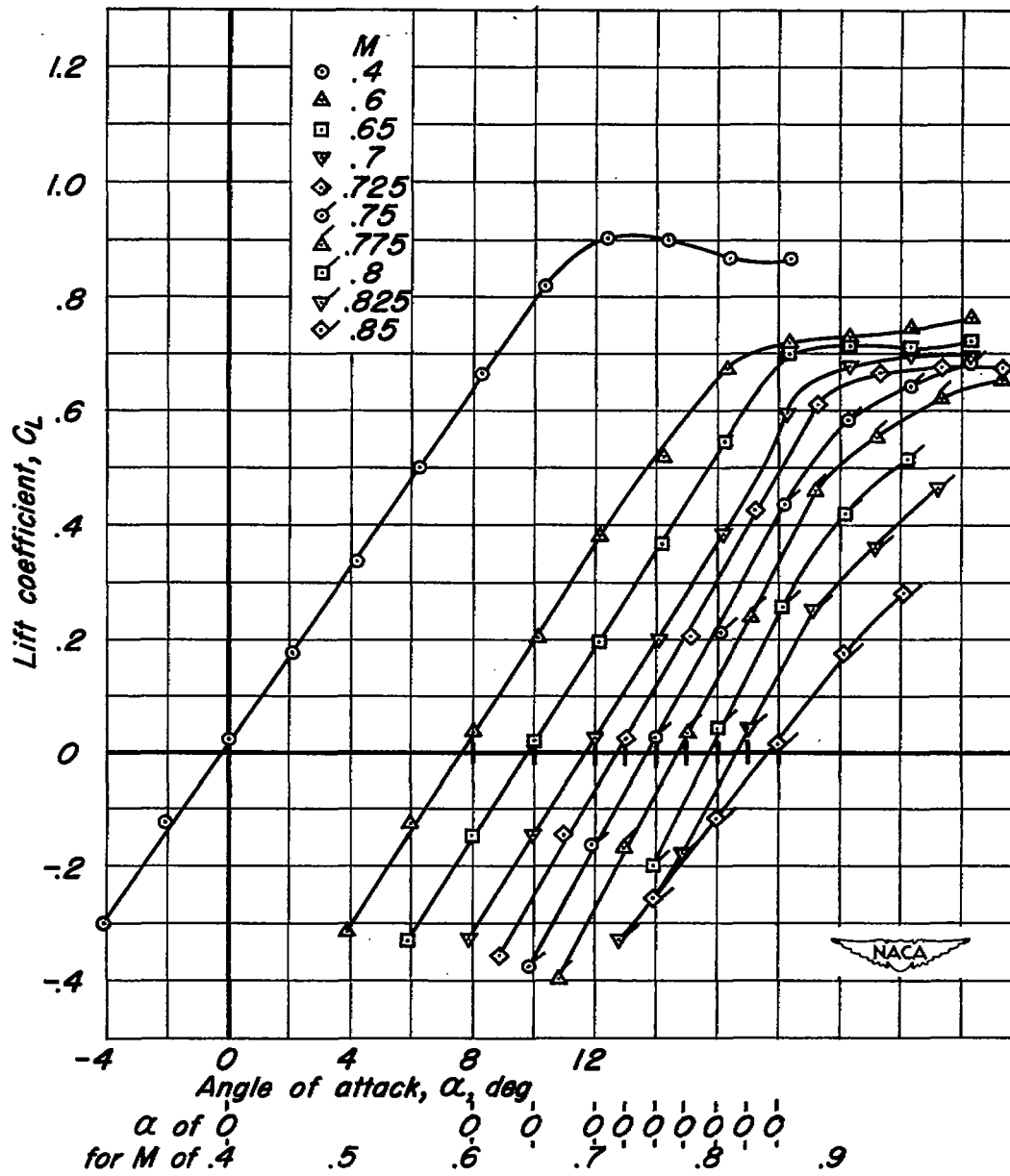


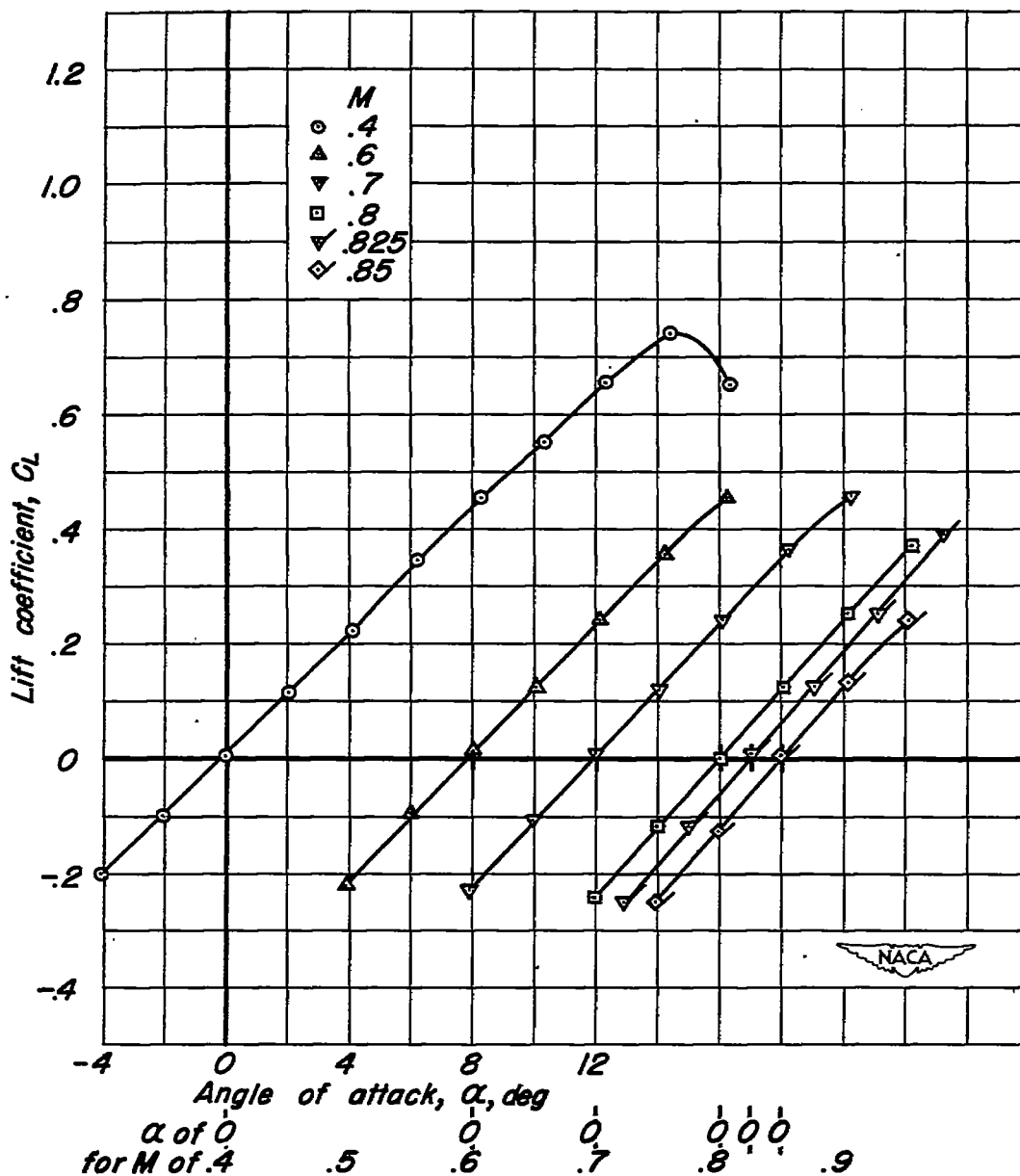
Figure 3.—Variation of Reynolds number with Mach number for the wing unswept and swept back 45°.



(a) Wing unswept

Figure 4.—Variation of lift coefficient with angle of attack.

Aileron undeflected.



(b) Wing swept back 45°

Figure 4. - Concluded.

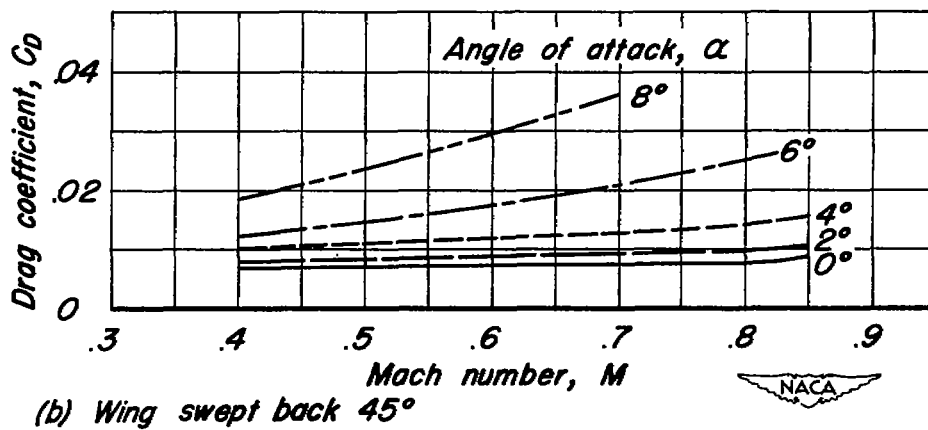
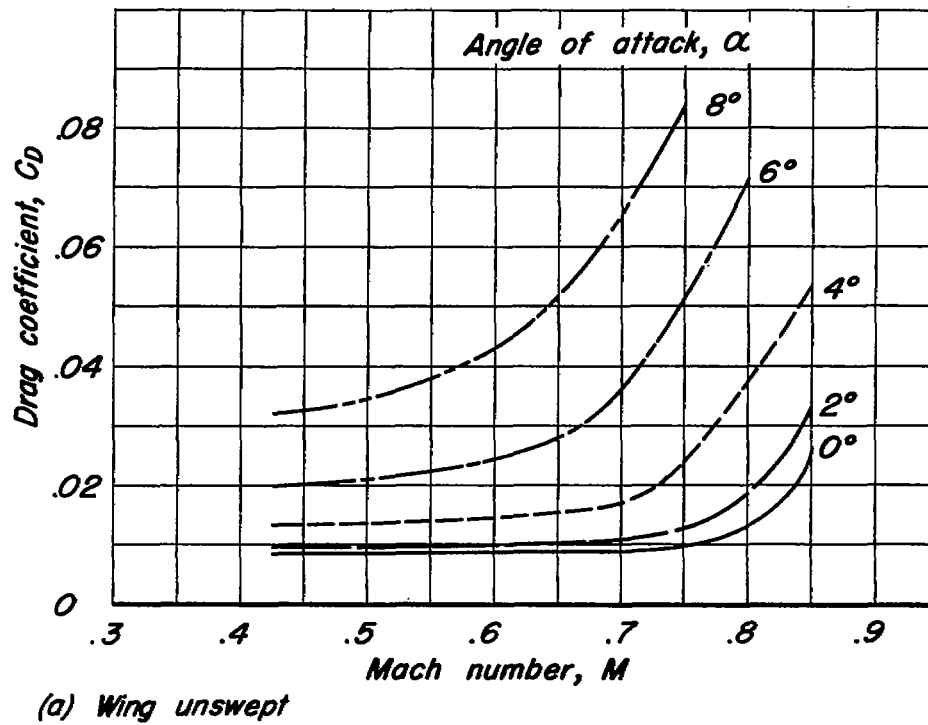
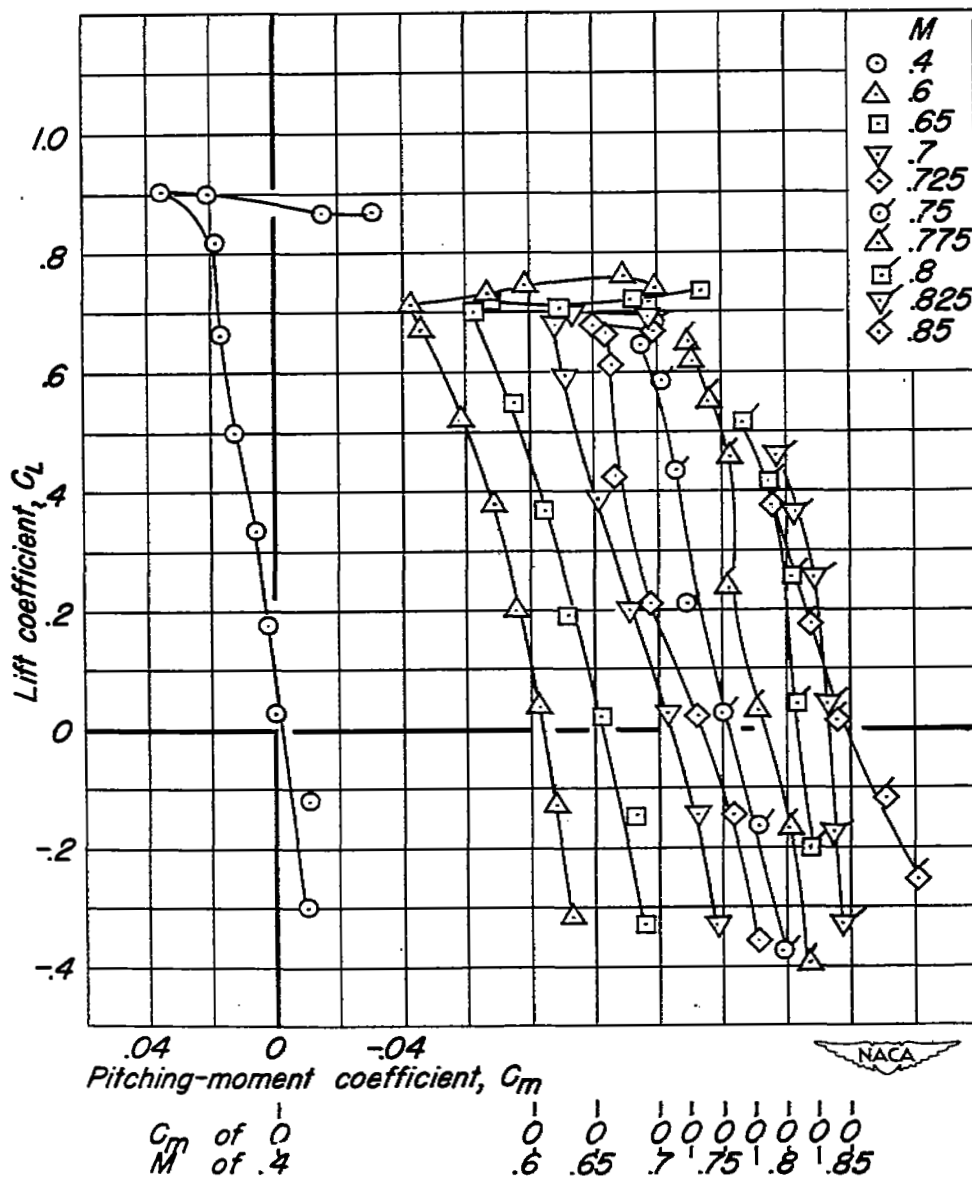
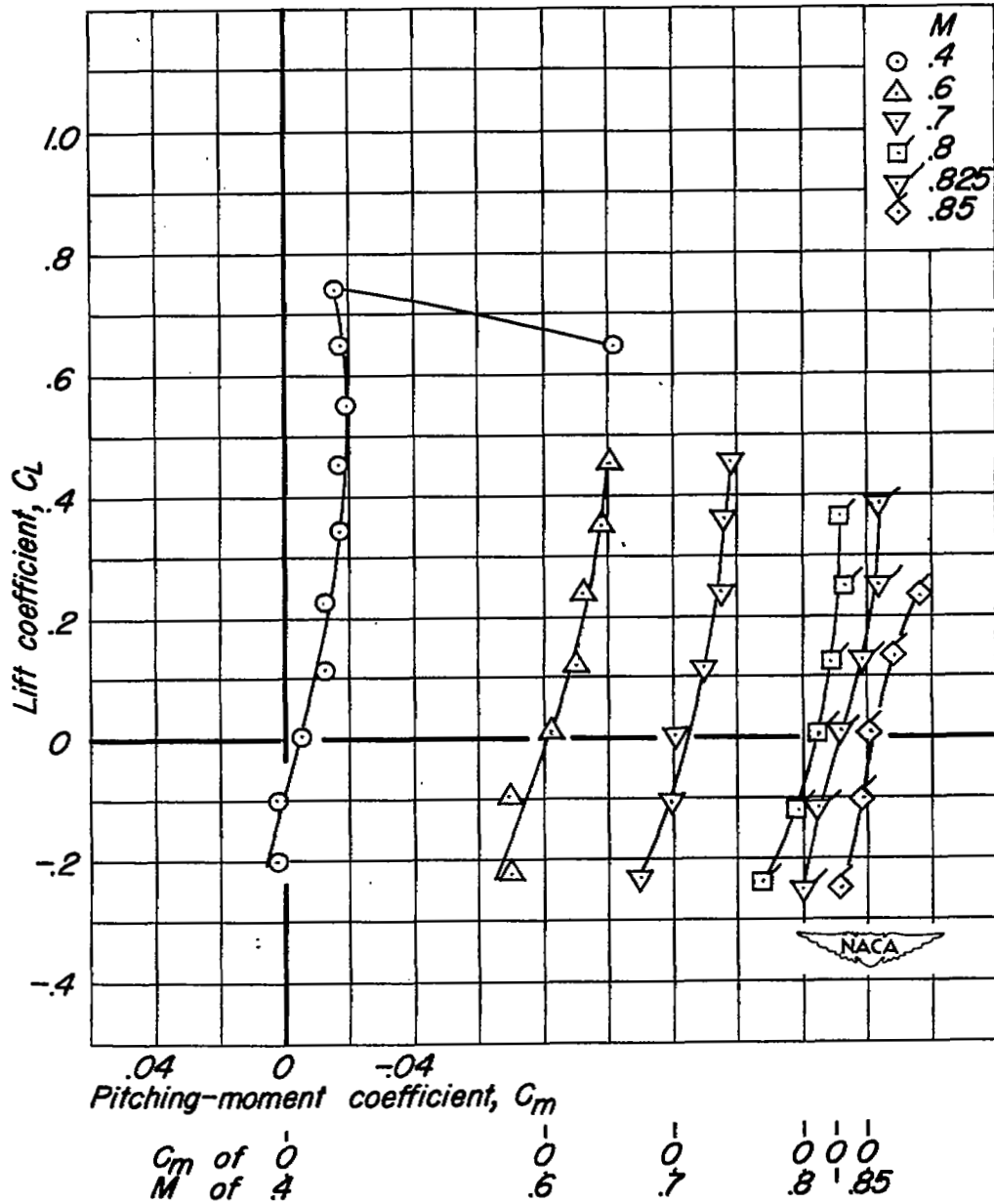


Figure 5. - Variation of drag coefficient with Mach number for constant angles of attack. Aileron undeflected.



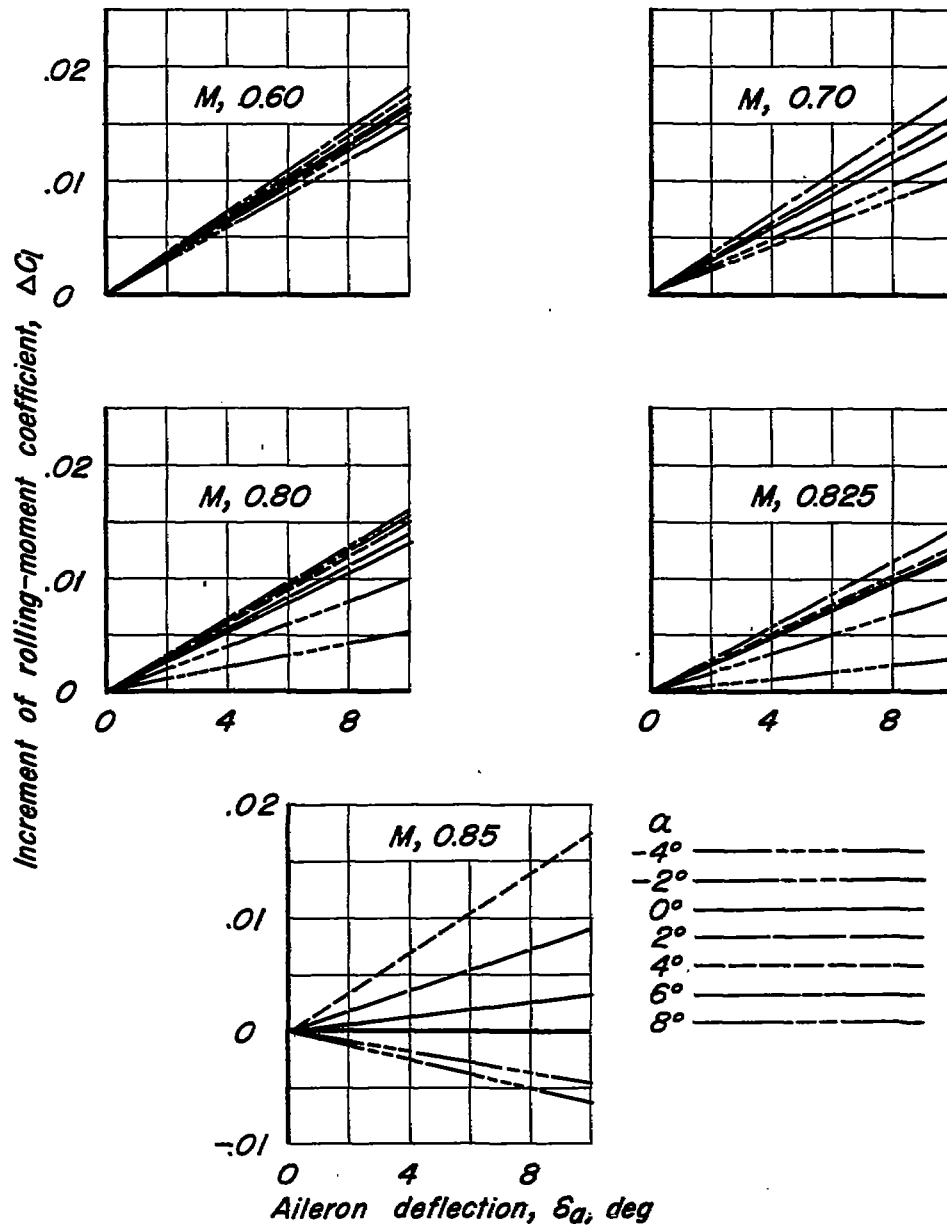
(a) Wing unswept.

Figure 6.—Variation of pitching-moment coefficient with lift coefficient. Aileron undeflected.



(b) Wing swept back 45°

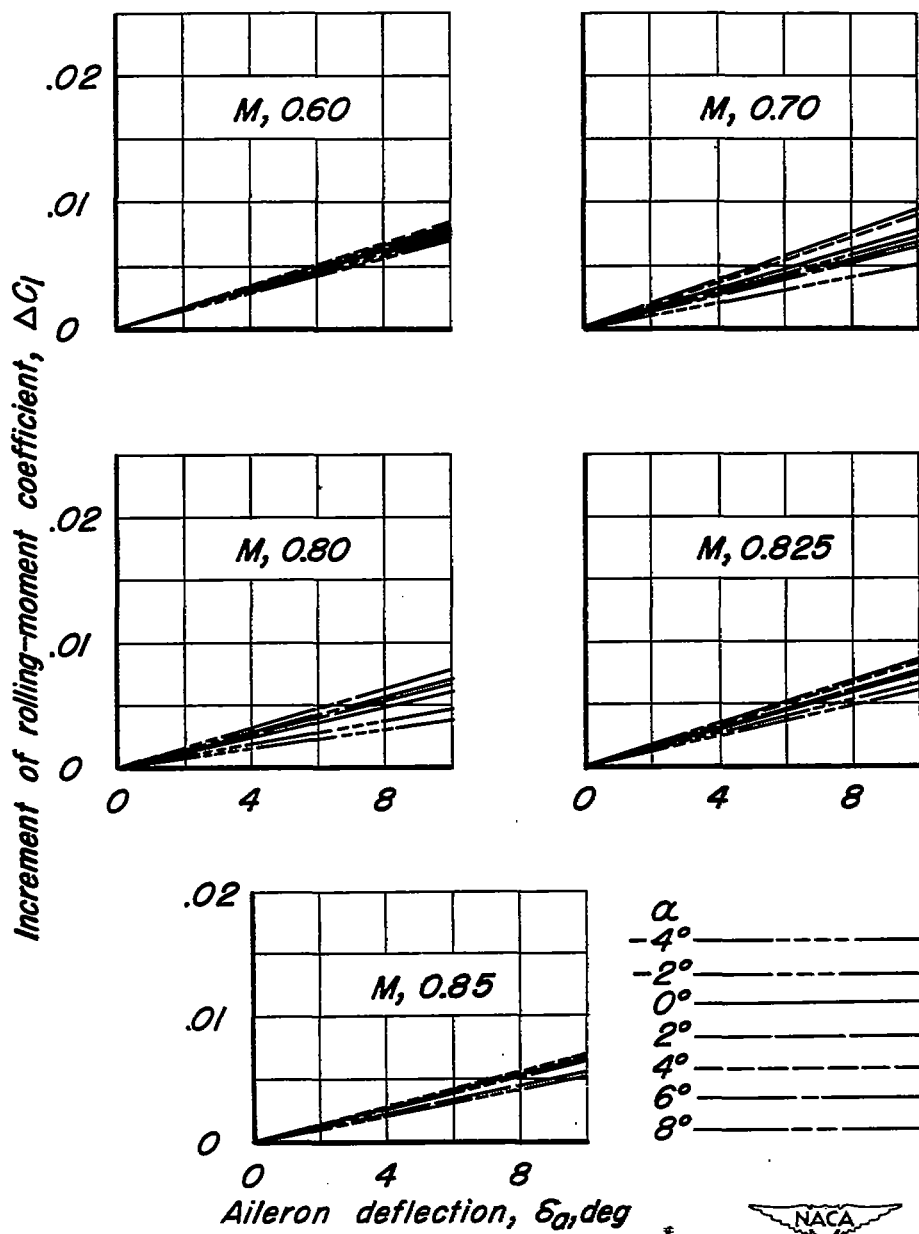
Figure 6.—Concluded.



(a) Wing unswept

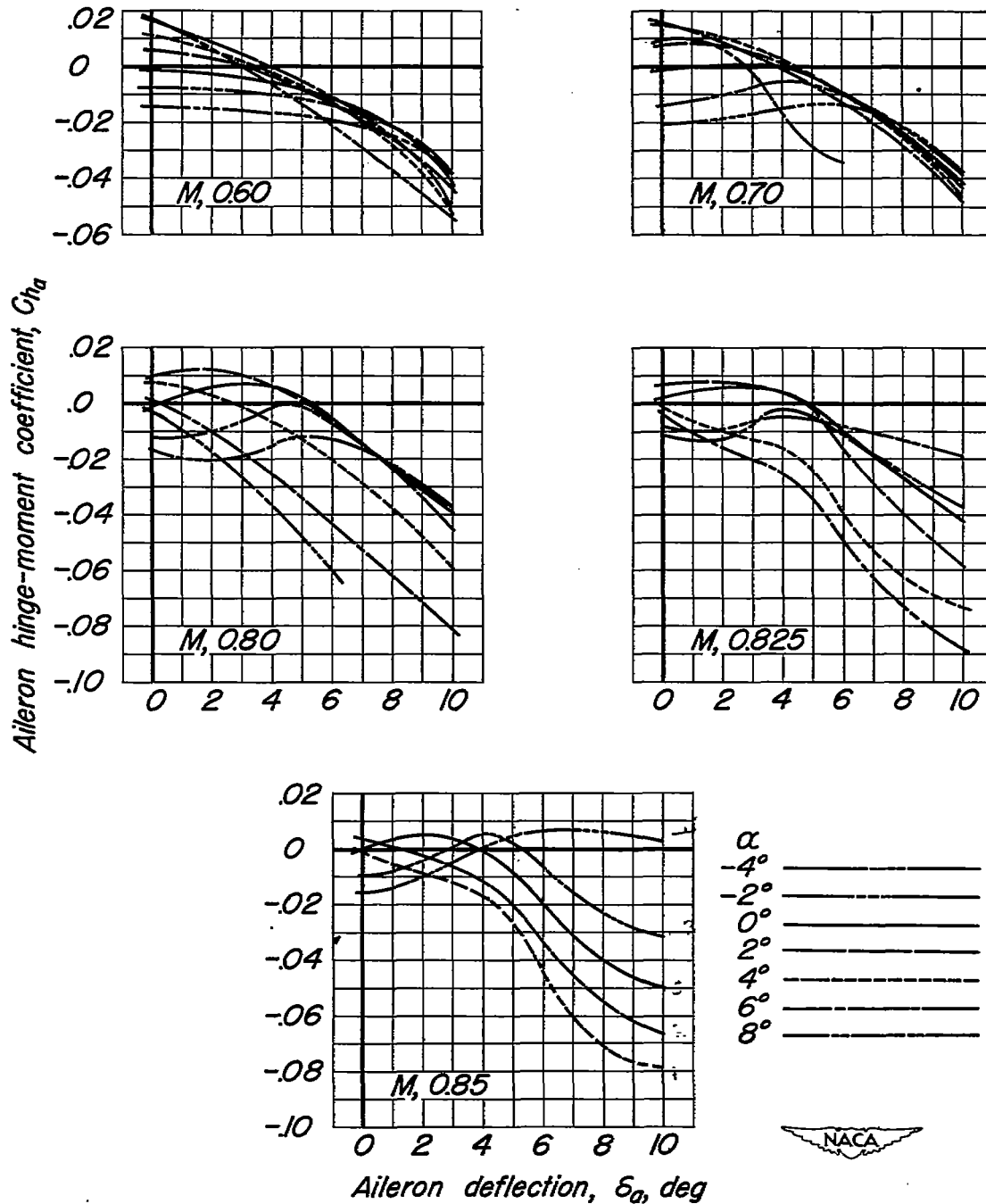


Figure 7.—Variation of increment of rolling-moment coefficient with trailing-edge aileron deflection.



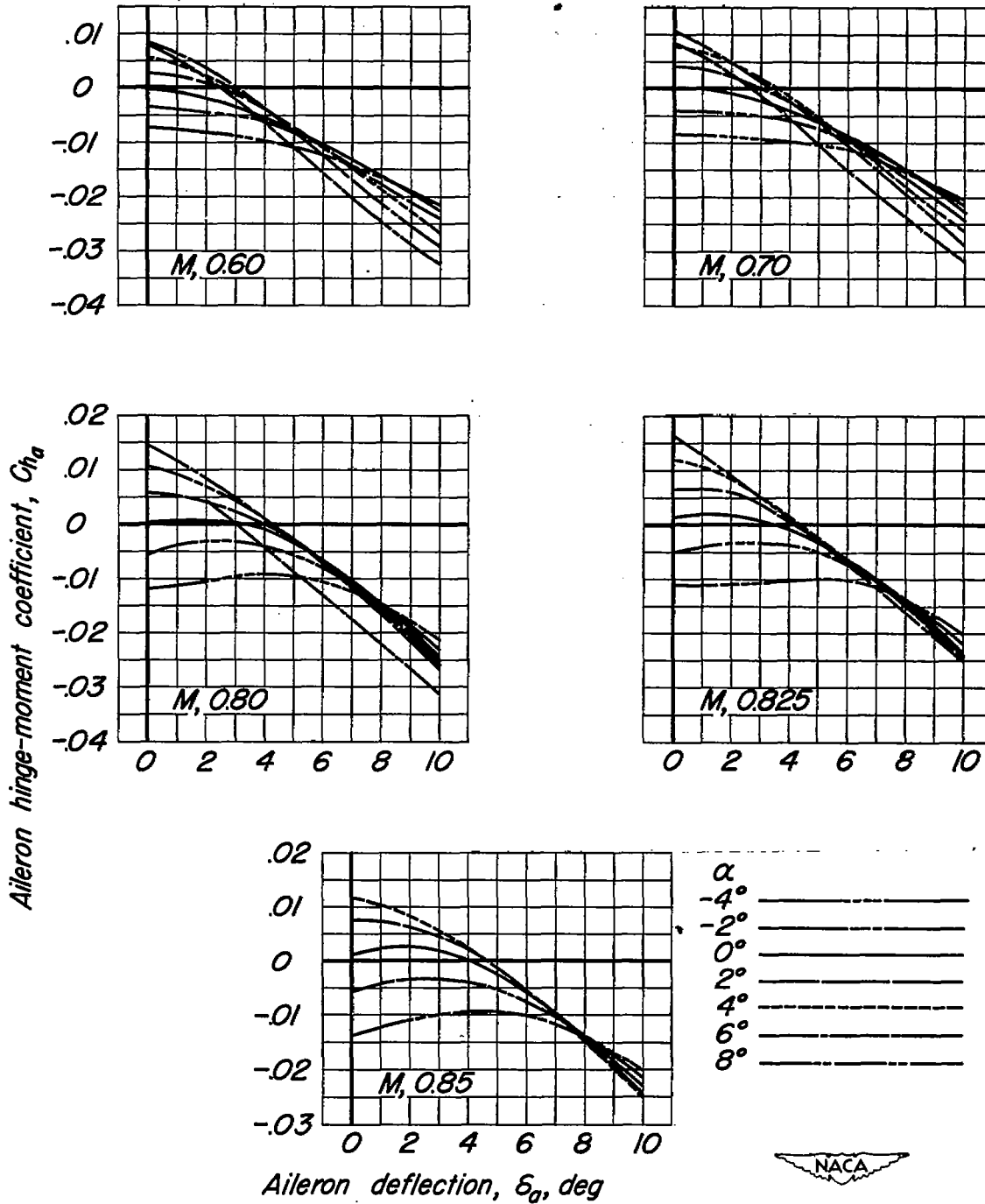
(b) Wing swept back 45°

Figure 7.—Concluded.



(a) Wing unswept

Figure 8.—Variation of trailing-edge aileron hinge-moment coefficient with aileron angle.



(b) Wing swept back 45°

Figure 8.—Concluded.

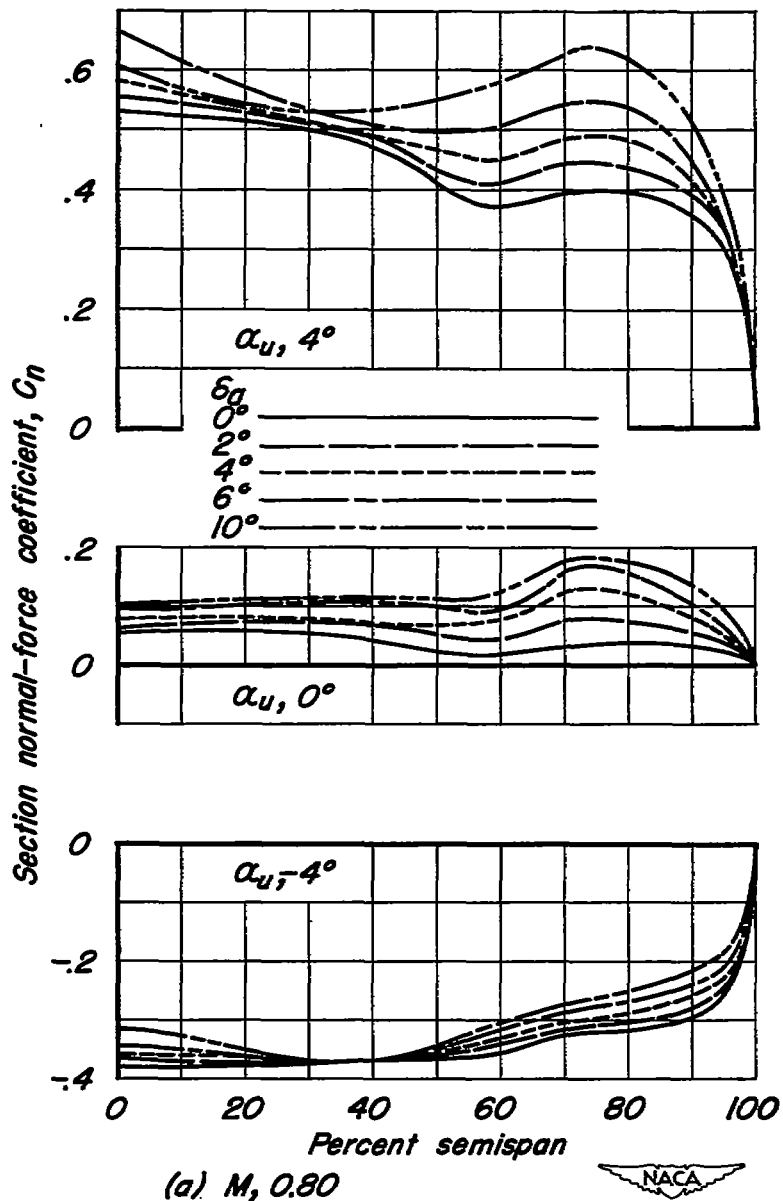


Figure 9.— Spanwise variation of section normal-force coefficient. Wing unswept.

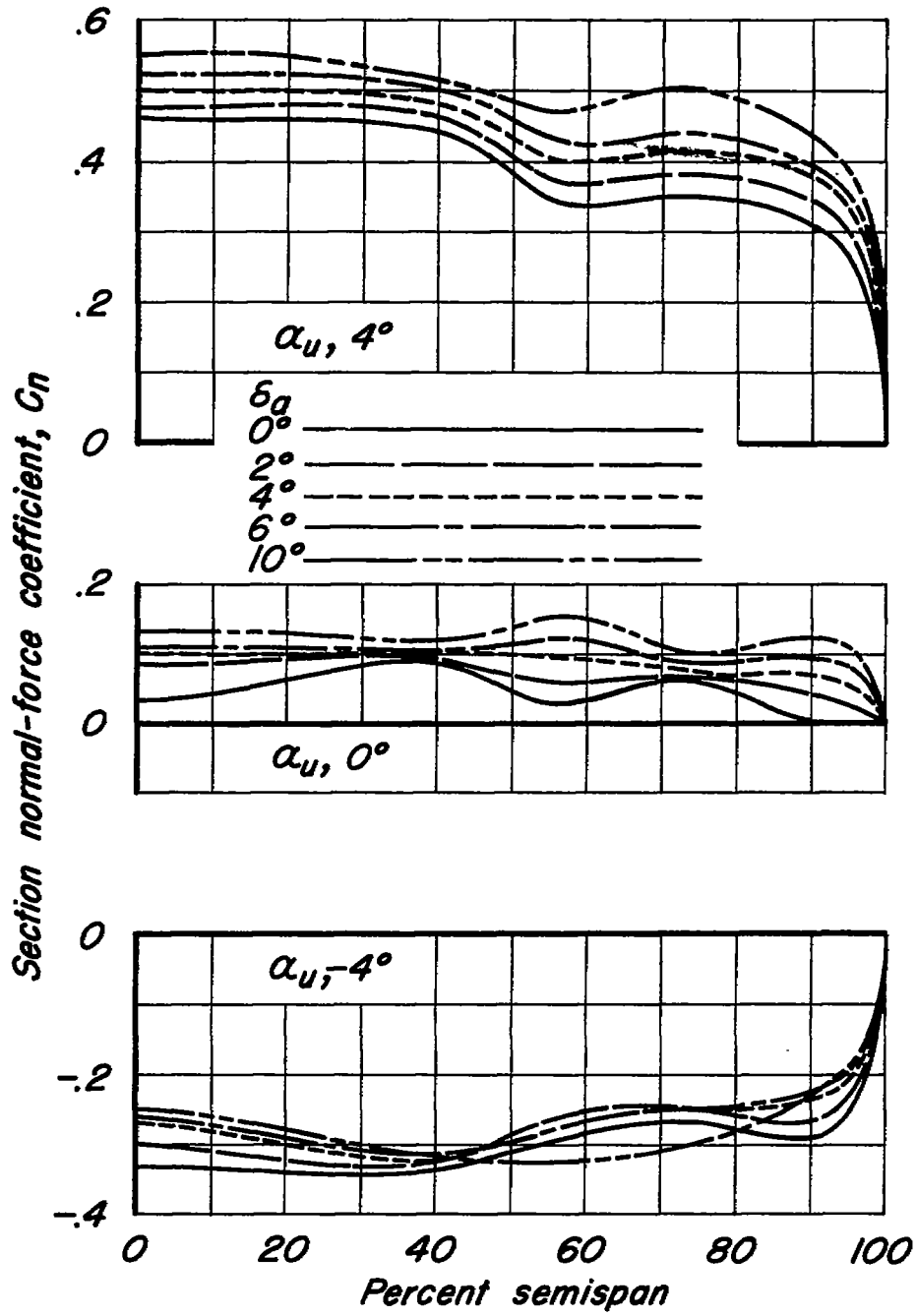
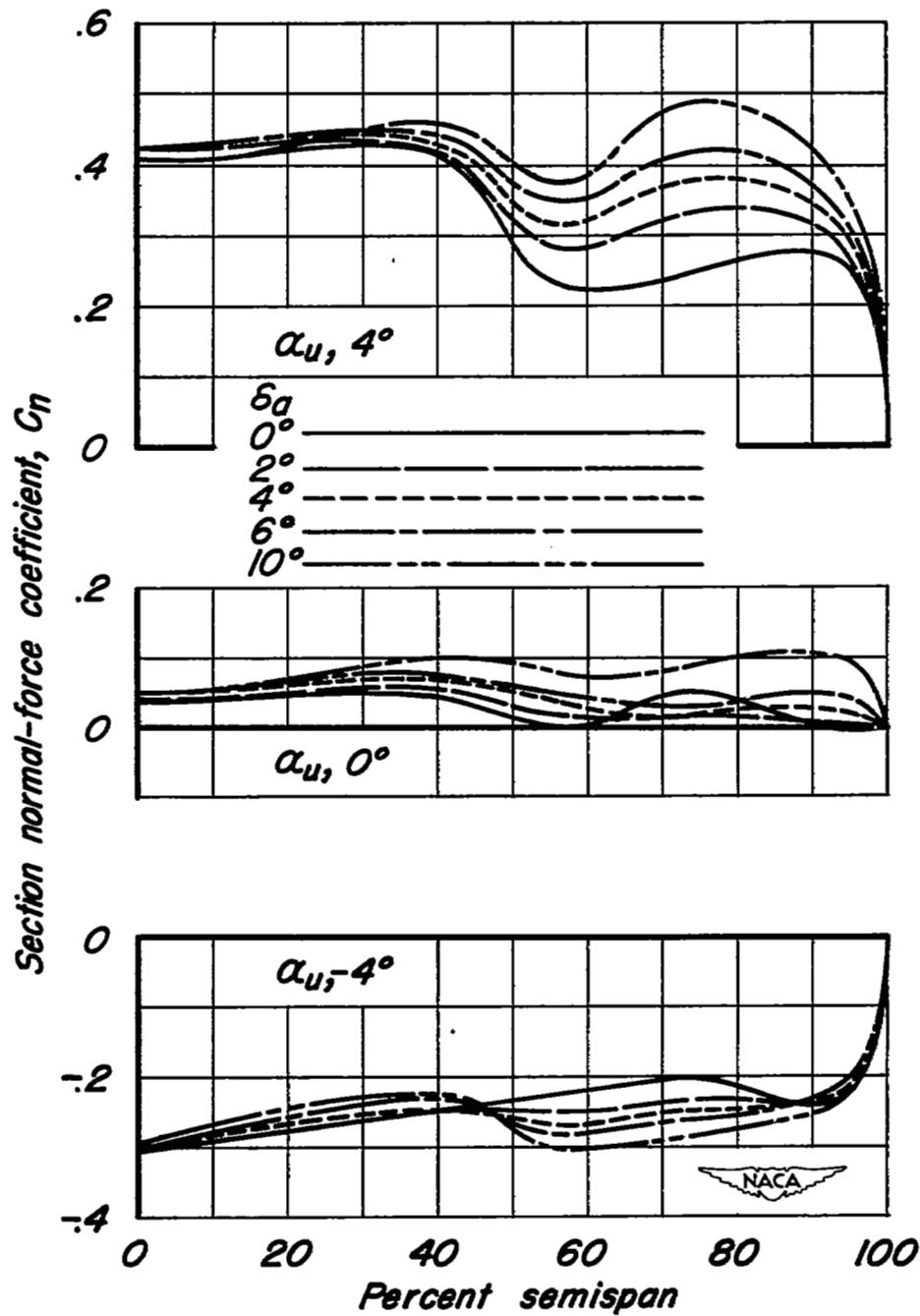
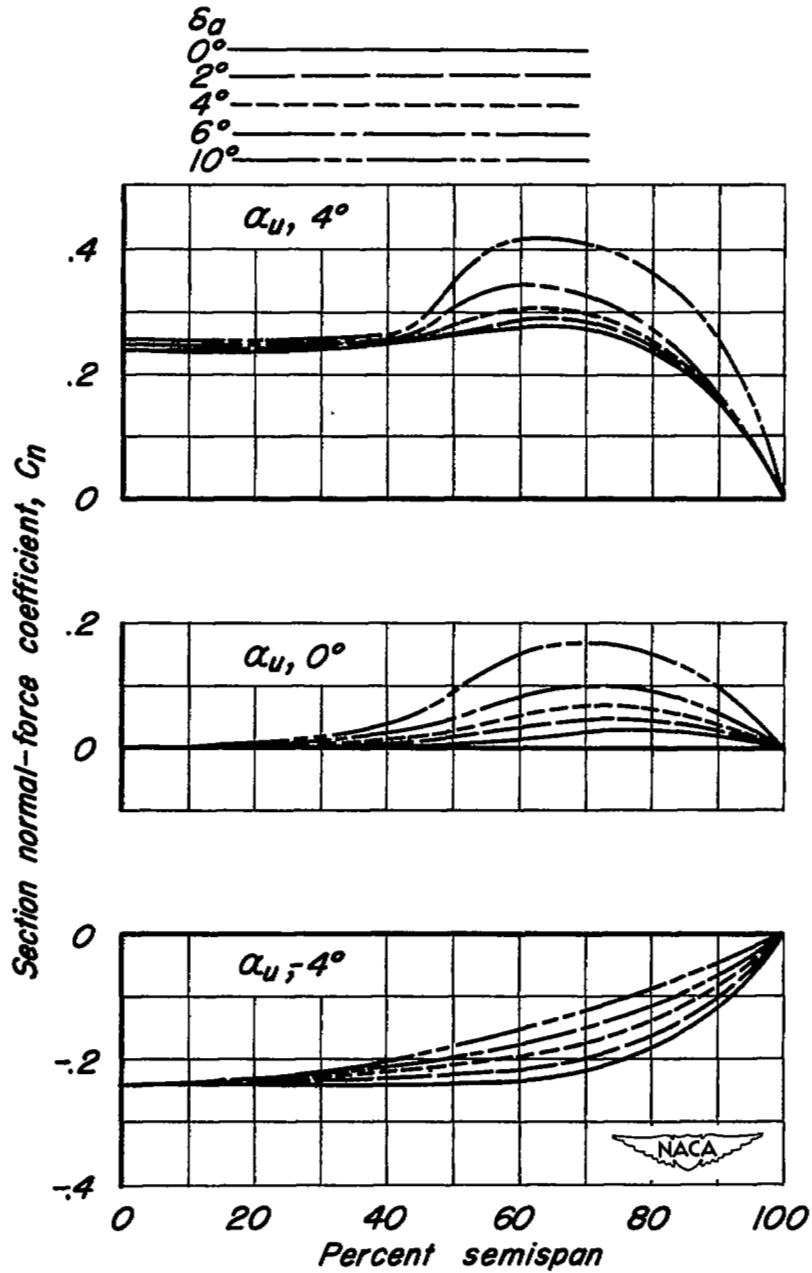
(b) $M, 0.825$ 

Figure 9.—Continued.



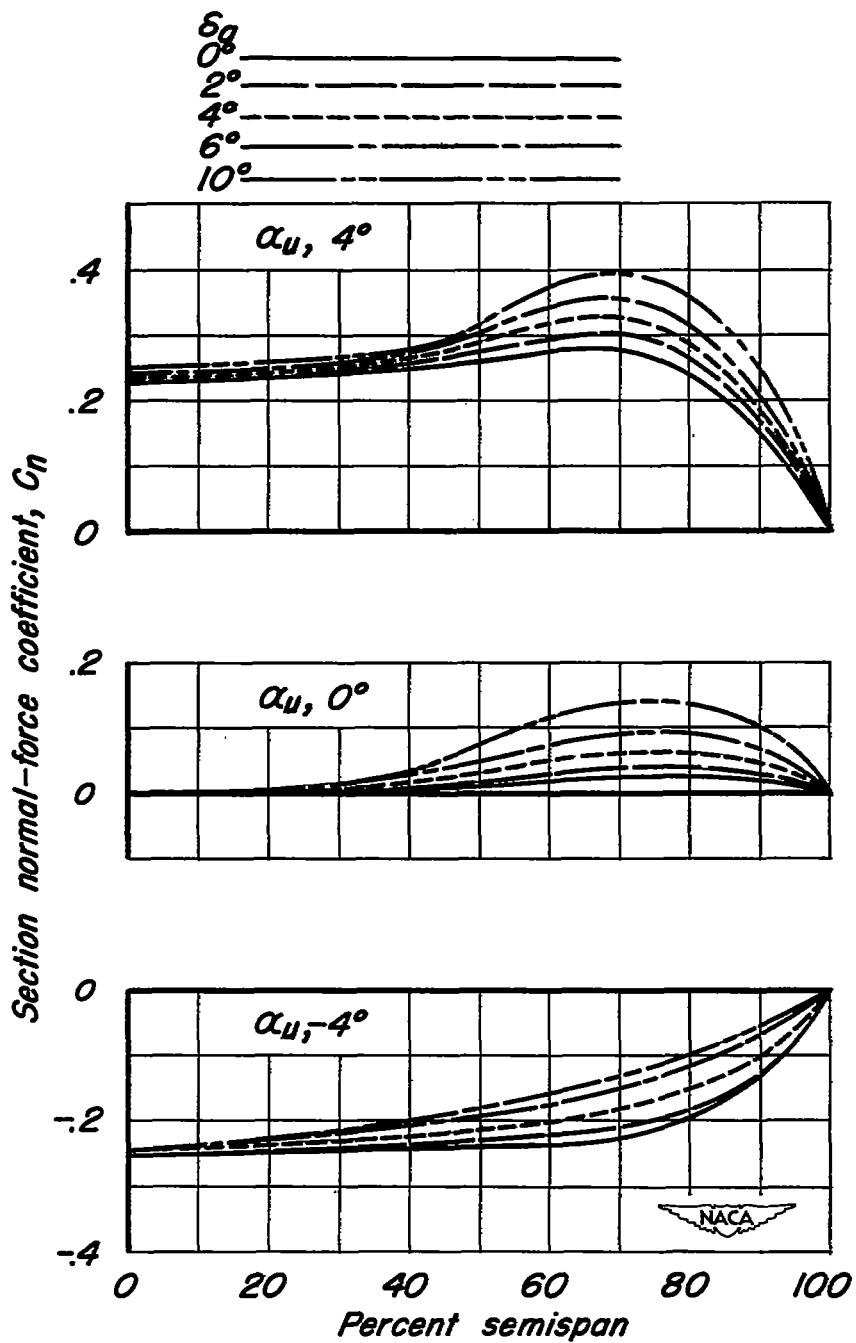
(c) $M, 0.85$

Figure 9. - Concluded.



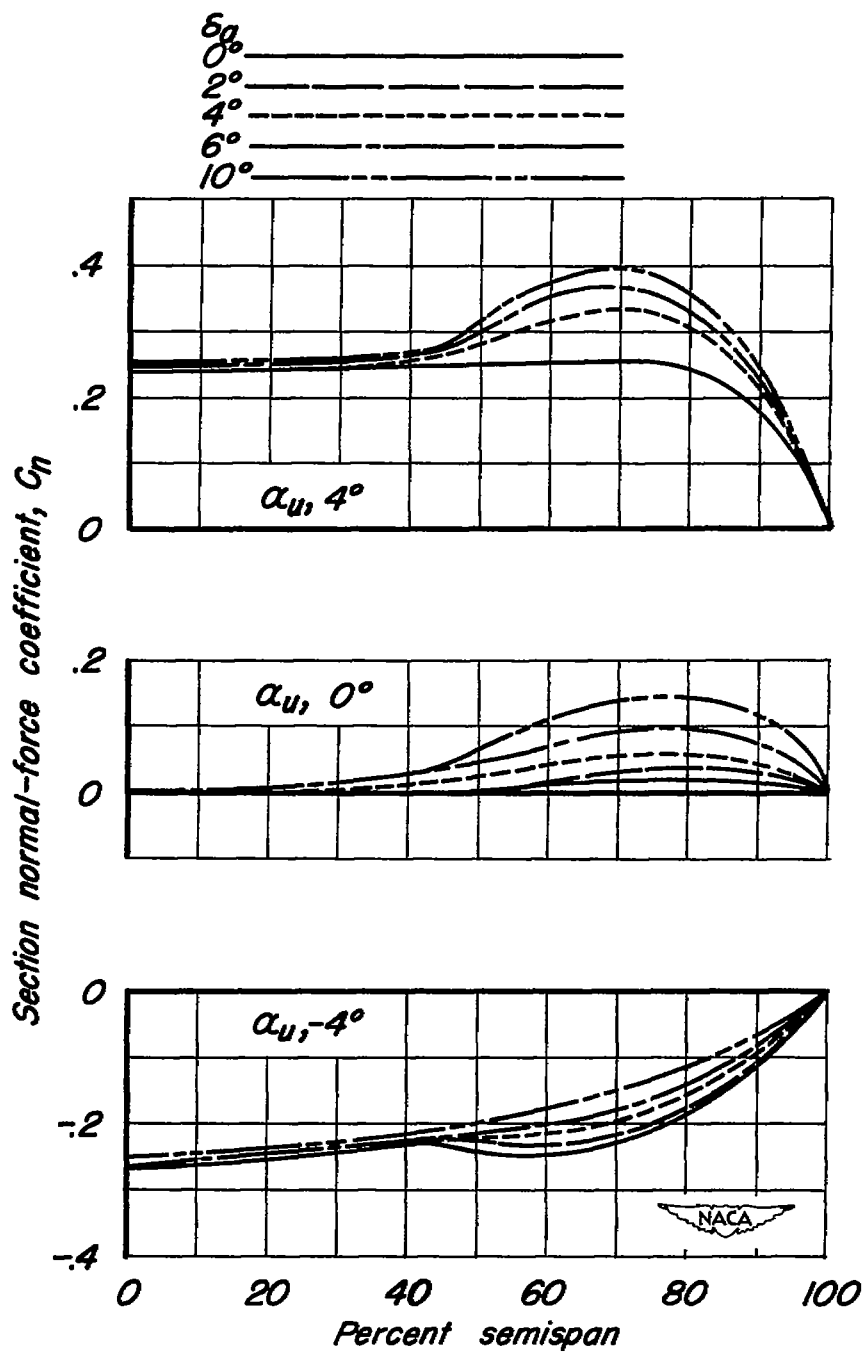
(a) $M, 0.80$

Figure 10.—Spanwise variation of section normal-force coefficient. Wing swept back 45° .



(b) $M, 0.825$

Figure 10.—Continued.



(c) $M, 0.85$

Figure 10.—Concluded.

NASA Technical Library



3 1176 01434 4619